Inorganic Chemistry

Article

pubs.acs.org/IC

Rhenium Complexes Based on 2-Pyridyl-1,2,3-triazole Ligands: A New Class of CO_2 Reduction Catalysts

H. Y. Vincent Ching,[†,‡,§,∥,⊥,#,∇] Xia Wang,[†] Menglan He,[‡,§] Noemi Perujo Holland,[‡,§] Régis Guillot,[○] Cyrine Slim,[∥,⊥,#,∇] Sophie Griveau,[∥,⊥,#,∇] Hélène C. Bertrand,[‡,§] Clotilde Policar,[*,‡,§] Fethi Bedioui,[*,∥,⊥,#,∇] and Marc Fontecave[*,†]

[†]Laboratoire de Chimie des Processus Biologiques, PSL Research University, Collège de France, CNRS UMR8229, Université Pierre et Marie Curie, 11 Place Marcelin Berthelot, 75231 Paris Cedex 05, France

[‡]Département de Chimie, Ecole Normale Supérieure, PSL Research University, UPMC Univ Paris 06, CNRS, Laboratoire des Biomolécules, 24 rue Lhomond, 75005 Paris, France

[§]Sorbonne Universités, UPMC Univ. Paris 06, Ecole Normale Supérieure, CNRS, Laboratoire des Biomolécules, 24 rue Lhomond, 75005 Paris, France

[∥]Chimie ParisTech, PSL Research University, Unité de Technologies Chimiques et Biologiques pour la Santé, F-75005 Paris, France

[⊥]CNRS, UTCBS UMR 8258, F-75006 Paris, France

[#]Université Paris Descartes, Sorbonne-Paris-Cité, UTCBS, F-75006 Paris, France

[∇]INSERM, UTCBS U 1022, F-75006 Paris, France

[○]Institut de Chimie Moléculaire et des Matériaux d'Orsay, Université Paris-Sud, UMR CNRS 8182, Université Paris-Saclay, 91405 Orsay, France

Supporting Information

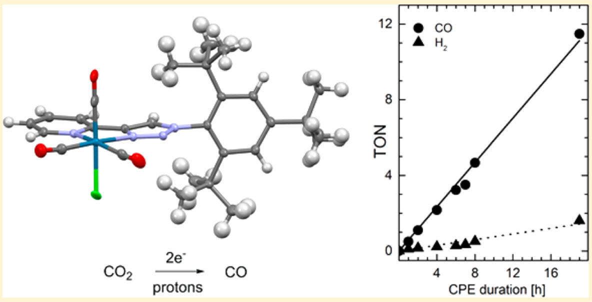

ABSTRACT: A series of $[Re(N^{\wedge}N)(CO)_3(X)]$ (N^N = diimine and X = halide) complexes based on 4-(2-pyridyl)-1,2,3-triazole (pyta) and 1-(2-pyridyl)-1,2,3-triazole (tapy) diimine ligands have been prepared and electrochemically characterized. The first ligand-based reduction process is shown to be highly sensitive to the nature of the isomer as well as to the substituents on the pyridyl ring, with the peak potential changing by up to 700 mV. The abilities of this class of complexes to catalyze the electroreduction and photoreduction of CO_2 were assessed for the first time. It is found that only Re pyta complexes that have a first reduction wave with a peak potential at ca. −1.7 V vs SCE are active, producing CO as the major product, together with small amounts of H_2 and formic acid. The catalytic wave that is observed in the CVs is enhanced by the addition of water or trifluoroethanol as a proton source. Long-term controlled potential electrolysis experiments gave total Faradaic yield close to 100%. In particular, functionalization of the triazolyl ring with a 2,4,6-tri-*tert*-butylphenyl group provided the catalyst with a remarkable stability.

INTRODUCTION

Carbon dioxide electroreduction into energy-dense carbon-based liquid or gaseous products is an attractive way to store renewable energies into chemical energy. However, because of the high stability of CO_2, its transformation implies multiple electron- and proton-transfers. Thus, catalysts are required for overcoming the slow kinetics, minimizing overpotentials, and controlling product selectivities. While solid metal-based catalysts are currently extensively investigated, homogeneous molecular metal complexes (coordination and organometallic complexes) provide unique opportunities to rationally address some of the issues discussed above, since their reactivity can be finely tuned via synthetic modifications of the ligands.[1−4] Furthermore, solid electrodes decorated with molecular complexes can be quite easily obtained using appropriately functionalized ligands and a variety of available methods for grafting them at the surface of conductive materials.[5−10] Surprisingly only a few classes of molecular electrocatalysts have been investigated since the 1980s with very limited structure−activity relationship studies. Compounds that have been receiving renewed attention include iron porphyrins,[11] on one hand, and polypyridine metal complexes (based on different metals such as Re, Ru, Ir, Rh, Mn, and Co), on the other.[4] The latter has indeed the ability to store multiple electrons across the entire molecule, not only at the metal center but also in the ligand π system, thus facilitating the reduction of CO_2. The prototypical catalyst from this second

Received: December 20, 2016

DOI: 10.1021/acs.inorgchem.6b03078

family is [2,2′-bipyridine]-chlorotricarbonylrhenium(I) ([Re(bpy)(Cl)$(CO)_3$]), as it has a high Faradaic efficiency for the generation of CO in the presence of Brønsted acids.[12] However, optimizing the system via modifications of the bpy ligand has been limited to a small number of functionalized bpys, with [Re(bpy-*t*Bu)(Cl)$(CO)_3$] (bpy-*t*Bu = 4,4′-di-*tert*-butyl-2,2′-bipyridine) being the most efficient catalyst to date.[13] This is in part due to the complexity of functionalizing the bpy ligand with moieties that can tune the electronic and steric of the metal complex, particularly in a dis-symmetric manner.[14,15]

To explore other classes of Re diimine complexes, using original diimines as alternative ligands to bpys, we investigated [Re(pyta)(X)$(CO)_3$] and [Re(tapy)(X)$(CO)_3$] complexes, in which pyta designates 4-(2-pyridyl)-1,2,3-triazole derivatives, while tapy designates 1-(2-pyridyl)-1,2,3-triazole derivatives, and X = Cl or Br (Scheme 1), as catalysts for CO_2 electroreduction. Not only can such ligands be easily prepared in good yields via a clean and efficient copper-catalyzed alkyne−azide cycloaddition (CuAAC) reaction (a widely used example of “click” chemistry)[16,17] but also this synthetic strategy allows controlled functionalization of both the pyridine and the triazole moieties and production of a great variety of ligands and complexes with finely tuned stereoelectronic properties. While some of the complexes studied here have been previously reported by us and found to display interesting luminescent properties,[17,18] a set of new pyta ligands and corresponding Re complexes are also reported here. The complexes have been evaluated for their electrocatalytic activity for CO_2 reduction, via rotating disk electrode (RDE) experiments, cyclic voltammetry (CV), and controlled potential electrolysis (CPE), as well as for their photocatalytic properties. To our knowledge this is the first structure−activity relationship study of a whole new class of electrocatalysts for CO_2 reduction based on such a large ensemble of molecules.

Scheme 1. Structure of the Ligands and Rhenium Complexes Synthesized and Investigated in This Study

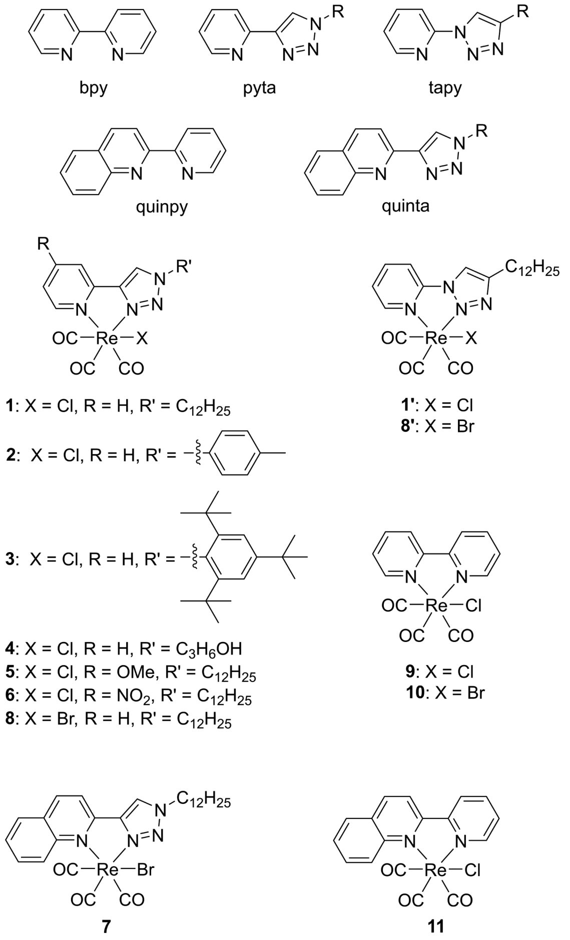

EXPERIMENTAL SECTION

Synthesis. *General Considerations.* ^1H and $^{13}C\{^1H\}$ NMR spectra were recorded on a Bruker Avance 300 or 400 spectrometers using residual solvent peaks as internal references. The following abbreviations are used: singlet (s), doublet (d), doublet of doublets (dd), triplet (t), doublet of triplets (td), quintuplet (quint), sextuplet (sext), and multiplet (m). Mass spectrometry (MS) services were performed at the ICMMO (Université Paris Sud, Orsay, France). The following abbreviations are used: MS, high-resolution mass spectrometry (HRMS), electrospray ionization (ESI), time-of-flight (TOF). Analytical reversed-phase high-performance liquid chromatography (HPLC) was performed on a Dionex Ultimate 3000 equipped with a variable wavelength detector, using a PROTO200 C18 3 μm 100 × 4.6 mm (Higgins Analytical Inc.) column. The results were analyzed using Chromeleon software. Thin-layer chromatography (TLC) analysis was performed on silica gel (Merck 60F-254) with visualization at 254 and 366 nm. Preparative flash chromatography was performed with Merck silica gel (Si 60, 40−63 μm). Reagents and chemicals were purchased from Sigma-Aldrich, Alfa Aesar, or Strem Chemicals and used without further purification. Anhydrous solvents (acetonitrile (MeCN), dichloromethane (DCM), dimethylformamide (DMF), tetrahydrofuran (THF), and toluene) were purchased from Sigma and used without further purification. IR spectra were recorded on a PerkinElmer Spectrum 100 FT-IR spectrometer. ***Caution!*** *Though no problem was encountered in the handling of any of the azides used, these compounds are potentially explosive and should thus be manipulated with caution.* [2-(1-Dodecyl-1*H*-1,2,3-triazol-4-yl)-pyridine]-chlorotricarbonylrhenium(I) (**1**), [3-(4-(pyridin-2-yl)-1*H*-1,2,3-triazol-1-yl)propan-1-ol]-chlorotricarbonylrhenium(I) (**4**), [2-(1-dodecyl-1,2,3-triazol-4-yl)-quinoline]-bromotricarbonylrhenium(I) (**7**), [2-(1-dodecyl-1*H*-1,2,3-triazol-4-yl)-pyridine]-bromotricarbonylrhenium(I) (**8**), [2-(4-dodecyl-1*H*-1,2,3-triazol-1-yl)pyridine]-chlorotricarbonylrhenium(I) (**1′**), and [2-(4-dodecyl-1*H*-1,2,3-triazol-1-yl)pyridine]-bromotricarbonylrhenium(I) (**8′**) were previously described by Bertrand et al.[17] [2,2′-Bipyridine]-chlorotricarbonylrhenium(I) (**9**) and [2,2′-bipyridine]-bromotricarbonylrhenium(I) (**10**) were prepared according to classical rhenium coordination procedures as described for the pyta complexes. 4-Azidotoluene was prepared according to Gjonaj and Roelfes,[19] dodecyl azide was prepared according to Juriček et al.,[20] and 1,3-dimethyl-2-phenyl-2,3-dihydro-1*H*-benzo[d]imidazole (BIH) was prepared according to Zhu et al.[21]

General Procedure A: Preparation of Rhenium Complexes. Chloropentacarbonylrhenium(I) (1.0 equiv) was dissolved in hot toluene (110 °C) under argon. The diimine ligand (1.1 equiv) was added, and the solution was refluxed overnight. The mixture was cooled to room temperature, and if a precipitate was formed, it was isolated by centrifugation, washed with cold toluene and cold diethyl ether, and dried in vacuo; otherwise, the solvent was evaporated, and the crude compound was purified by column chromatography. The purification protocols for each complex are described below.

2-(1-(p-Tolyl)-1H-1,2,3-triazol-4-yl)pyridine. 4-Azidotoluene (333 mg, 2.5 mmol, 1.0 equiv) and 2-ethynylpyridine (250 mg, 2.5 mmol, 1.0 equiv) were dissolved in 1:1 DCM/water (10 mL) mixture. Copper(II) sulfate pentahydrate (62 mg, 0.25 mmol, 0.1 equiv) and sodium ascorbate (100 mg, 0.5 mmol, 0.2 equiv) in water (1 mL) were added to the mixture. After it was stirred overnight at room temperature under argon, more copper(II) sulfate pentahydrate (62 mg, 0.25 mmol, 0.1 equiv) and sodium ascorbate (100 mg, 0.5 mmol, 0.2 equiv) in water (1 mL) were added. After it was stirred for 48 h, DCM (50 mL) was added to the mixture. The organic phase was decanted, and aqueous ammonium hydroxide (20 mL, 0.1 M) and sodium ethylenediaminetetraacetate (20 mL, 0.1 M) solutions were added to the aqueous phase. The aqueous phase was extracted with DCM (3 × 50 mL). The organic phases were combined, dried over sodium sulfate, filtered, and evaporated. The residue was purified by column chromatography on silica gel (eluent 3:2 cyclohexane/ethyl acetate) to yield a pale yellow solid (270 mg, 48% chemical yield). Characterizations were in accordance with those published in Bolje et al.[22]

*[2-(1-(p-Tolyl)-1H-1,2,3-triazol-4-yl)pyridine]-chlorotricarbonylrhenium(I) (**2**).* This complex was obtained following the general procedure A starting from 2-[1-(*p*-tolyl)-1*H*-1,2,3-triazol-4-yl]pyridine (74 mg, 0.31 mmol, 1.1 equiv). The desired product precipitated as a pale yellow solid (154 mg, quantitative).

^{1}H NMR (300 MHz, CD_3CN): δ (ppm) 9.06 (s, 1H), 9.00 (ddd, J = 5.5, 1.4, 0.8 Hz, 1H), 8.18 (ddd, J = 7.9, 7.8, 1.4 Hz, 1H), 8.08 (ddd, J = 7.9, 1.4, 0.8 Hz, 1H), 7.78 (m, 2H), 7.55 (ddd, J = 7.8, 5.5, 1.4 Hz, 1H), 7.49 (m, 2H), 2.46 (s, 3H). ^{13}C{^{1}H} NMR (75 MHz, CD_3CN): δ (ppm) 154.2, 150.3, 150.0, 142.2, 141.5, 131.6, 127.4, 124.2, 123.5, 121.9, 21.3. MS (ESI+) m/z (%): 525.0544 (100) $[M - Cl + water]^+$, 507.0435 (75) $[M - Cl]^+$, 565.0011 (25) $[M + Na]^+$. HRMS (ESI+) calcd for $C_{17}H_{12}ClN_4NaO_3Re$ 565.0039, found 565.0011. HPLC (50 to 100% MeCN in 10 min): retention time (rt) 4.94 (>95%). IR: ν_{max}/cm^{-1} 2027, 1943, 1920, 1892 (CO).

2,4,6-Tri-tert-butylphenylazide. 2,4,6-Tri-*tert*-butylaniline (400 mg, 1.5 mmol, 1.0 equiv) was dissolved in anhydrous MeCN (4 mL) under argon. The solution was cooled to 0 °C, and *tert*-butyl nitrite (274 μL, 2.3 mmol, 1.5 equiv) was added dropwise, followed by azidotrimethylsilane (238 μL, 1.8 mmol, 1.2 equiv) dropwise. After the solution was stirred overnight at room temperature, the solvent was evaporated to dryness, and the residue was purified by column chromatography on silica gel (eluent 2:1 cyclohexane/DCM) to yield a white crystalline solid (313 mg, 75% chemical yield)).

R_f (2:1 cyclohexane/DCM) = 0.93. ^{1}H NMR (300 MHz, $CDCl_3$): δ (ppm) 7.35 (s, 2H), 1.48 (s, 18H), 1.32 (s, 9H). ^{13}C{^{1}H} NMR (75 MHz, $CDCl_3$): δ (ppm) 148.3, 145.3, 134.9, 122.5, 36.2, 35.0, 31.4, 31.3. MS (ESI+) m/z (%): 260.2370 (100) $[M\text{-}N_2 + H]^+$. HRMS (ESI+) calcd for $C_{18}H_{30}N$ 260.2378, found 260.2370.

2-(1-(2,4,6-Tri-tert-butylphenyl)-1H-1,2,3-triazol-4-yl)pyridine. 2,4,6-Tri-*tert*-butylphenylazide (50.0 mg, 0.17 mmol, 1.0 equiv) and 2-ethynylpyridine (18.0 mg, 0.17 mmol, 1.0 equiv) were dissolved in 1:1 DCM/water (4 mL) mixture. Copper(II) sulfate pentahydrate (4.3 mg, 0.017 mmol, 0.1 equiv) and sodium ascorbate (6.8 mg, 0.035 mmol, 0.2 equiv) in water (0.5 mL) were added to the mixture. After it was stirred for 48 h, DCM (10 mL) was added to the mixture. The organic phase was decanted out and aqueous ammonium hydroxide (10 mL, 0.1 M) and sodium ethylenediaminetetraacetate (10 mL, 0.1 M) solutions were added to the aqueous phase. The aqueous phase was extracted with DCM (3 × 10 mL). The organic phases were combined, dried over sodium sulfate, filtered and evaporated. The residue was purified by column chromatography on silica gel (eluent 4:1 cyclohexane/ethyl acetate) to yield a white crystalline solid (30 mg, 45% chemical yield).

R_f (4:1 cyclohexane/ethyl acetate) = 0.53. ^{1}H NMR (300 MHz, $CDCl_3$): δ (ppm) 8.61 (ddd, J = 4.8, 1.7, 1.0 Hz, 1H), 8.33 (s, 1H), 8.29 (dt, J = 7.9, 1.0 Hz, 1H), 7.81 (td, J = 7.9, 1.7 Hz, 1H), 7.57 (s, 2H), 7.27 (td, J = 4.8, 1.0 Hz, 1H), 1.38 (s, 9H), 1.01 (s, 18H). ^{13}C{^{1}H} NMR (75 MHz, $CDCl_3$): δ (ppm) 152.0, 150.3, 149.5, 147.5, 147.1, 136.9, 131.7, 129.1, 123.7, 122.9, 120.4, 36.9, 35.3, 32.2, 31.3. MS (ESI+) m/z (%): 391.2857 (100) $[M + H]^+$, 413.2671 (30) $[M + Na]^+$. HRMS (ESI+) calcd for $C_{25}H_{35}N_4$ 391.2856, found 391.2857.

*[2-(1-(2,4,6-Tri-tert-butylphenyl)-1H-1,2,3-triazol-4-yl)pyridine]-chlorotricarbonylrhenium(I) (**3**).* This complex was obtained following the general procedure A starting from 2-[1-(2,4,6-tri-*tert*-butylphenyl)-1*H*-1,2,3-triazol-4-yl]pyridine (14 mg, 0.036 mmol, 1.1 equiv). The desired product precipitated as a cream solid (20 mg, 85% chemical yield).

^{1}H NMR (300 MHz, DMSO-d_6): δ (ppm) 9.76 (s, 1H), 9.01 (m, 1H), 8.33 (m, 2H), 7.77 (m, 1H), 7.63 (s, 2H), 1.37 (s, 9H), 1.07 (s, 9H), 1.05 (s, 9H). ^{13}C{^{1}H} NMR (75 MHz, DMSO-d_6): δ (ppm) 153.3, 153.0, 148.2, 147.8, 147.0, 146.8, 140.9, 132.0, 129.9, 126.9, 124.0, 123.9, 122.8, 36.5, 36.4, 35.0, 31.9. MS (ESI+) m/z (%): 719.1761 (100) $[M + Na]^+$. HRMS (ESI+) calcd for $C_{28}H_{34}ClN_4NaO_3Re$ 719.1761, found 719.1761. HPLC (80 to 100% MeCN in 10 min): rt 4.77 (>95%). IR: ν_{max}/cm^{-1} 2023, 1925, 1883, 1868 (CO).

4-Nitro-2-(trimethylsilyl)ethynyl)pyridine. 2-Bromo-4-nitropyridine (437.0 mg, 2.15 mmol, 1.0 equiv) was dissolved with DMF (3.0 mL) and Et_3N (1.0 mL). The mixture was bubbled with argon for 15 min. Bis(triphenylphosphine)palladium(II) dichloride (16.6 mg, 0.0236 mmol, 1.1 mol %) and CuI (1.7 mg, 0.0086 mmol, 0.4 mol %) were added under an atmosphere of argon, followed by trimethylsilylacetylene (365 μL, 2.58 mmol, 1.2 equiv). The mixture was stirred at 60 °C under argon for 4 h. The mixture was diluted with DCM and washed with saturated aqueous ammonium chloride solution (2×) and saturated brine. The organic phase was dried over sodium sulfate, filtered, and evaporated. The residue was purified by column chromatography on silica gel (eluent 9:1 cyclohexane/ethyl acetate) to afford the product as a pale brown solid (395.0 mg, 83% chemical yield). Characterizations were in accordance with those published in Carlsson et al.[23]

2-Ethynyl-4-methoxypyridine. 4-Nitro-2-(trimethylsilyl)ethynyl)-pyridine (375.0 mg, 1.7 mmol, 1.0 equiv) was dissolved in methanol (30.0 mL), and potassium carbonate (247.0 mg, 1.79 mmol, 1.05 equiv) was added. The mixture was stirred at room temperature under argon for 3 h. The mixture was diluted wih DCM and water and extracted with DCM (2×). The combined organic phases were dried over sodium sulfate, filtered, and evaporated. The residue was purified by column chromatography on silica gel (eluent 7:3 cyclohexane/ethyl acetate) to afford 2-ethynyl-4-methoxypyridine as a brown oil (166.0 mg, 73% chemical yield). Characterizations were in accordance with those published in Carlsson et al.[23]

2-(1-Dodecyl-1H-1,2,3-triazol-4-yl)-4-methoxypyridine. 2-Ethynyl-4-methoxypyridine (21.0 mg, 0.16 mmol, 1.0 equiv) and 1-azidododecane (36.0 mg, 0.17 mmol, 1.05 equiv) were dissolved in a mixture of DCM (1.0 mL) and water (0.6 mL). Copper(II) sulfate pentahydrate (4.0 mg, 0.016 mmol, 0.1 equiv) and sodium ascorbate (9.0 mg, 0.048 mmol, 0.3 equiv) were added under argon, and the mixture was stirred at room temperature for 23 h. The mixture was diluted with DCM and water and decanted. The organic phase was dried over sodium sulfate, filtered, and evaporated. The residue was purified by column chromatography (eluent ethyl acetate) to afford 2-(1-dodecyl-1*H*-1,2,3-triazol-4-yl)-4-methoxypyridine as a white solid (30.3 mg, 55% chemical yield).

R_f (eluent ethyl acetate) = 0.71. ^{1}H NMR (300 MHz, $CDCl_3$): δ (ppm): 8.37 (d, J = 5.8 Hz, 1H), 8.21 (s, 1H), 7.76 (d, J = 2.6 Hz, 1H), 6.78 (dd, J = 5.8, 2.6 Hz, 1H), 4.40 (t, J = 7.2 Hz, 2H), 3.94 (s, 3H), 1.94 (quint, J = 7.6 Hz, 2H), 1.51−1.10 (m, 18H), 0.86 (t, J = 6.0 Hz, 3H). ^{13}C{^{1}H} NMR (75 MHz, $CDCl_3$): δ (ppm): 166.9, 151.8, 150.0, 147.8, 122.4, 110.5, 105.3, 55.6, 50.7, 32.0, 30.4, 29.7, 29.6, 29.5, 29.45, 29.1, 26.6, 22.8, 14.2. MS (ESI+) m/z (%): 345.2652 (100) $[M + H]^+$. HRMS (ESI+) calcd for $C_{20}H_{33}N_4O$ 345.2654, found 345.2652.

*[2-(1-Dodecyl-1H-1,2,3-triazol-4-yl)-4-methoxypyridine]-chlorotricarbonylrhenium(I) (**5**).* This complex was obtained following the general procedure A starting from 2-(1-dodecyl-1*H*-1,2,3-triazol-4-yl)-4-methoxypyridine (24 mg, 0.07 mmol, 1.0 equiv). The residue was dried under reduced pressure and purified by column chromatography on silica gel (eluent ethyl acetate) to yield the product as a pale yellow solid (41.7 mg, 92% chemical yield).

^{1}H NMR (300 MHz, $CDCl_3$): δ (ppm): 8.70 (d, J = 6.4 Hz, 1H), 8.41 (s, 1H), 7.35 (d, J = 2.7 Hz, 1H), 6.86 (dd, J = 6.4, 2.7 Hz, 1H), 4.39−4.23 (m, 1H), 4.14−3.98 (m, 1H), 3.91 (s, 3H), 1.93−1.82 (m, 2H), 1.46−1.16 (m, 18H), 0.87 (t, J = 7.5 Hz, 3H). ^{13}C{^{1}H} NMR (75 MHz, $CDCl_3$): δ (ppm): 167.8, 153.8, 151.3, 149.1, 124.4, 113.1, 107.3, 57.4, 52.3, 32.0, 30.1, 29.7, 29.6, 29.5, 29.4, 29.0, 26.5, 22.8, 14.3. MS (ESI+) m/z (%): 673.1538 (100) $[M + Na]^+$. HRMS (ESI+): calcd for $C_{23}H_{32}ClN_4NaO_4Re$ 673.1567, found 673.1538. HPLC (80 to 100% ACN in 10 min): rt 6.15 (>95%). IR: ν_{max}/cm^{-1} 2019, 1885 (CO).

4-Nitro-2-(triisopropylsilyl)ethynyl)pyridine. 2-Bromo-4-nitropyridine (150.0 mg, 0.74 mmol, 1.0 equiv) was dissolved with DMF (2.0 mL) and Et_3N (0.1 mL). The mixture was bubbled with argon for 15 min. Bis(triphenylphosphine)palladium(II) dichloride (11.0 mg, 0.015 mmol, 2 mol %) and CuI (1.4 mg, 0.0071 mmol, 1 mol %) were added under an atmosphere of argon, followed by triisopropylsilylacetylene (0.2 mL, 0.89 mmol, 1.2 equiv). The mixture was stirred at room temperature under argon for 30 h. The mixture was filtered and evaporated to dryness, and the residue was purified by column chromatography on silica gel (eluent 10:1 cyclohexane/ethyl acetate) to afford 4-nitro-2-(triisopropylsilyl)ethynyl)pyridine as a yellow liquid, (99.8 mg, 44% chemical yield), which was used directly in the next step.

2-Ethynyl-4-nitropyridine. 4-Nitro-2-(triisopropylsilyl)ethynyl)-pyridine (99.8 mg, 0.33 mmol, 1.0 equiv) was dissolved in 2.0 mL of THF and cooled at 0 °C. Tetrabutylammoniumfluoride, (TBAF; 0.31 mL, 0.31 mmol, 0.95 equiv, 1 M in THF) was added, and the mixture was stirred at 0 °C under argon for 30 min. The mixture was diluted wih water and extracted with DCM. The organic phase was dried over sodium sulfate, filtered, and evaporated. The residue was purified by column chromatography on silica gel (eluent 7:3 cyclohexane/ethyl acetate) to afford 2-ethynyl-4-nitropyridine as a beige solid (37.2 mg, 76% chemical yield). Characterizations were in accordance with those published in Carlsson et al.[23]

2-(1-Dodecyl-1H-1,2,3-triazol-4-yl)-4-nitropyridine. 2-Ethynyl-4-nitropyridine (37.0 mg, 0.25 mmol, 1.0 equiv) and 1-azidododecane (58.0 mg, 0.28 mmol, 1.05 equiv) were dissolved in a mixture of DCM (2.0 mL) and water (1.5 mL); copper(II) sulfate pentahydrate (8.0 mg, 0.03 mmol, 0.12 equiv) and sodium ascorbate (16.0 mg, 0.08 mmol, 0.36 equiv) were added under argon, and the mixture was stirred at room temperature for 16 h. The mixture was diluted with DCM and water and decanted. The organic phase was dried over sodium sulfate, filtered, and evaporated. The residue was purified by column chromatography (eluent 7:3 cyclohexane/ethyl acetate) to afford 2-(1-dodecyl-1*H*-1,2,3-triazol-4-yl)-4-nitropyridine (79.0 mg, 88% chemical yield.)

R_f (eluent 7:3 cyclohexane/ethyl acetate) = 0.39. ^{1}H NMR (300 MHz, $CDCl_3$): δ (ppm): 8.89 (d, J = 2.2 Hz, 1H), 8.85 (d, J = 5.4 Hz, 1H), 8.21 (s, 1H), 7.93 (dd, J = 5.4, 2.2 Hz, 1H), 4.45 (t, J = 7.2 Hz, 2H), 1.97 (quint, J = 7.0 Hz, 2H), 1.52−1.11 (m, 18H), 0.87 (t, J = 6.0 Hz, 3H). ^{13}C{^{1}H} NMR (75 MHz, $CDCl_3$): δ (ppm): 154.9, 153.6, 151.6, 146.7, 123.0, 115.0, 113.0, 50.9, 32.0, 30.4, 29.7, 29.6, 29.5, 29.46, 29.1, 26.6, 22.8, 14.25. MS (ESI+) m/z (%): 382.2222 (100) [M + Na]$^+$. HRMS (ESI+) calcd for $C_{19}H_{29}N_5NaO_2$ 382.2219, found 382.2222.

*[2-(1-Dodecyl-1H-1,2,3-triazol-4-yl)-4-nitropyridine]-chlorotricarbonylrhenium(I) (**6**).* This complex was obtained following the general procedure A starting from 2-(1-dodecyl-1*H*-1,2,3-triazol-4-yl)-4-nitropyridine (30 mg, 0.08 mmol, 1.0 equiv). The residue was dried under reduced pressure and purified by column chromatography on silica gel (eluent 1:1 cyclohexane/ethyl acetate) to yield the product as an orange solid (55.5 mg, quantitative chemical yield).

^{1}H NMR (300 MHz, acetone-d_6): δ (ppm): 9.42 (dd, J = 6.1, 0.7 Hz, 1H), 9.39 (s, 1H), 9.00 (dd, J = 2.4, 0.7 Hz, 1H), 8.35 (dd, J = 6.1, 2.4 Hz, 1H), 4.76 (t, J = 7.2 Hz, 2H), 2.21−2.06 (m, 2H), 1.53−1.13 (m, 18H), 0.86 (t, J = 6.0 Hz, 3H). ^{13}C{^{1}H} NMR (75 MHz, acetone-d_6): δ (ppm): 156.6, 156.2, 153.3, 148.6, 127.5, 119.7, 116.6, 53.1, 32.6, 30.4, 30.2, 30.1, 30.06, 29.6, 26.9, 23.3, 14.35. MS (ESI+) m/z (%): 688.1285 (100) [M + Na]$^+$. HRMS (ESI+): calcd for $C_{22}H_{29}ClN_5NaO_5Re$ 688.1312, found 688.1285. HPLC (80 to 100% ACN in 10 min): rt 6.03 (>95%). IR: ν_{max}/cm^{-1} 2023, 1897 (CO).

2-Pyridin-2-yl-quinoline. 2-Chloroquinoline (303.0 mg, 1.852 mmol, 1.0 equiv) and 2-(tributylstannyl)pyridine (600.0 μL, 1.852 mmol, 1.0 equiv) were added to degassed anhydrous DMF (3.9 mL). The mixture was degassed with argon for 5 min, bis(triphenylphosphine)palladium(II) dichloride (130.0 mg, 0.185 mmol, 0.1 equiv) was added, and the mixture was stirred at 110 °C for 24 h under argon. The mixture was diluted with water (20 mL) and Et_2O (20 mL) and filtered over diatomaceous earth, and the diatomaceous earth was washed with Et_2O (2 × 25 mL). The filtrate was washed with water (3 × 25 mL) and saturated brine (3 × 25 mL). Combined organic phases were dried over sodium sulfate and filtered, and the solvent was removed in vacuo. The crude product was purified by column chromatography on silica gel (eluent 7:3 cyclohexane/ethyl acetate) to afford the product as pale yellow crystals (159 mg, 42% chemical yield).

R_f (7:3 cyclohexane/ethyl acetate) = 0.64. ^{1}H NMR (400 MHz, $CDCl_3$): δ (ppm): 8.75 (d, J = 4.8 Hz, 1H), 8.66 (d, J = 8.0 Hz, 1H), 8.57 (d, J = 8.8 Hz, 1H), 8.23 (d, J = 8.8 Hz, 1H), 8.19 (d, J = 8.4 Hz, 1H), 7.92−7.84 (m, 2H), 7.74 (t, J = 7.6 Hz, 1H), 7.56 (t, J = 7.6, 1H), 7.39−7.33 (m, 1H). ^{13}C{^{1}H} NMR (100 MHz, $CDCl_3$): δ (ppm): 156.2, 156.0, 149.0, 147.8, 136.8, 136.6, 129.7, 129.4, 128.1, 127.4, 126.6, 123.8, 121.7, 118.8. HRMS (ESI+): calcd for $C_{14}H_{11}N_2$ ([M + H]$^+$) 207.0917, found 207.0194; calcd for $C_{14}H_{10}N_2Na$ ([M+Na$^+$]$^+$) 229.0736, found 229.0732.

*[2-Pyridin-2-yl-quinoline]-chlorotricarbonylrhenium(I) (**11**).* This complex was obtained following the general procedure A starting from 2-pyridin-2-yl-quinoline (30.3 mg, 0.155 mmol, 1.0 equiv). The residue was dried under reduced pressure and purified by column chromatography on silica gel (eluent 5:5 cyclohexane/ethyl acetate) to yield a bright orange solid (44.2 mg, 56% chemical yield).

R_f (eluent ethyl acetate) = 0.40. ^{1}H NMR (300 MHz, acetone d-6): δ (ppm): 9.29 (d, J = 5.1 Hz, 1H), 8.97−8.81 (m, 3H), 8.75 (d, J = 8.7 Hz, 1H), 8.41 (t, J = 7.6 Hz, 1H), 8.23 (d, J = 8.4 Hz, 1H), 8.13 (t, J = 8.4 Hz, 1H), 7.88 (q, J = 7.4 Hz, 2H). ^{13}C{^{1}H} NMR (75 MHz, acetone d-6): δ (ppm): 159.7, 158.3, 154.1, 148.4, 142.2, 141.0, 133.6, 131.4, 130.2, 128.7, 126.7, 121.0. HRMS (ESI+): calcd for $C_{17}H_{10}ClN_2NaO_3Re$ ([M + Na]$^+$) 534.9821, found 534.9807. HPLC (50 to 100% ACN in 10 min): rt 4.19 (>95%). IR: ν_{max}/cm^{-1} 2015, 1891, 1860 (CO).

Crystallography. X-ray diffraction data were collected by using a Kappa X8 APPEX II Bruker diffractometer with graphite-monochromated Mo Kα radiation (λ = 0.710 73 Å). Crystals were mounted on a CryoLoop (Hampton Research) with Paratone-N (Hampton Research) as cryoprotectant and then flash-frozen in a nitrogen-gas stream at 100 K. The temperature of the crystal was maintained at the selected value (100 K) by means of a 700 series Cryostream cooling device to within an accuracy of ±1 K. The data were corrected for Lorentz polarization and absorption effects. The structures were solved by direct methods using SHELXS-97[24] and refined against F^2 by full-matrix least-squares techniques using SHELXL-97[25] with anisotropic displacement parameters for all non-hydrogen atoms. Hydrogen atoms were located on a difference Fourier map and introduced into the calculations as a riding model with isotropic thermal parameters. All calculations were performed by using the Crystal structure crystallographic software package WINGX.[26] Additional crystallographic information is available in the Supporting Information.

Electrochemistry. Rotating disk and cyclic voltammetry were performed with a classical three-electrode single compartment cell at room temperature, using a glassy carbon disk working electrode (3 mm diameter, Origalys, France), a Pt wire counter electrode, and a Ag/AgCl wire pseudoreference electrode. The experiments were performed using a VSP Potentiostat (Bio-Logic, France). Fc/Fc$^+$ (0.46 V vs saturated calomel electrode (SCE)) was used as an internal standard. The working electrode was polished with 1200 grit and then 2400 grit SiC papers, and at the start of each experiment with 3 and 0.3 μm diamond pastes followed by extensive rinsing and sonication with ultrapure water and ethanol. With the same set up, microelectrode voltammetry was performed using a microcarbon fiber electrode (33 μm dia., IJ Cambria Scientific Ltd., U.K.) instead of the 3 mm disk electrode. IR drop was compensated to 75% using the ZIR built-in compensation method of the Bio-Logic potentiostat. MeCN solutions containing 0.1 M Bu_4NPF_6 as the supporting electrolyte were deaerated with Ar or saturated with CO_2 for at least 10 min before cyclic voltammograms (CVs) were recorded.

Controlled-potential electrolysis experiments were performed at room temperature in a custom-built, gas-tight two-compartment electrochemical cell. The cathodic compartment, which contained a fitting for a 15 mm diameter glassy carbon disk working electrode, was

Scheme 2. Synthesis[a] of Complexes 2, 3, 5, and 6

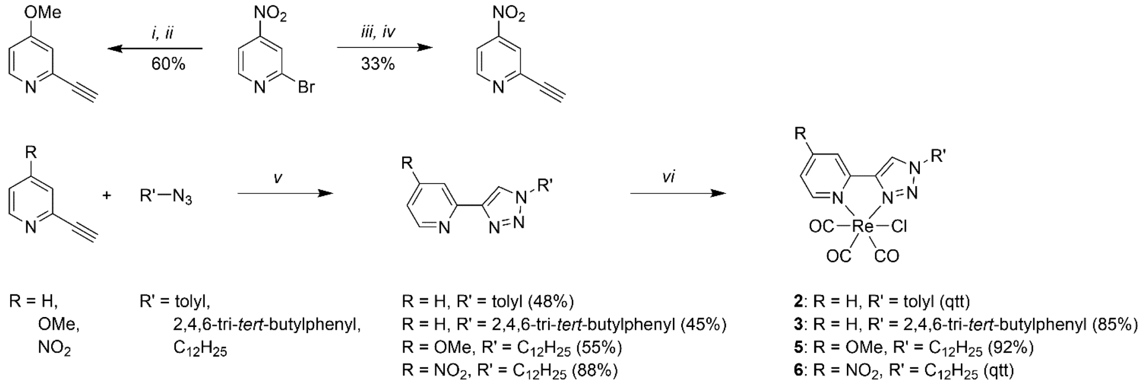

[a](i) Trimethylsilylacetylene (1.2 equiv), CuI (0.4 mol %), $Pd(PPh_3)Cl_2$ (1.1 mol %), DMF, Et_3N, 60 °C, 4 h, 83%; (ii) K_2CO_3 (1.05 equiv), MeOH 73%; (iii) triisopropylsilylacetylene (1.2 equiv), CuI (1 mol %), $Pd(PPh_3)Cl_2$ (2 mol %), DMF, Et_3N, room temperature, 30 h, 44%; (iv) TBAF (0.95 equiv), THF, 0 °C, 76%; (v) $CuSO_4.5H_2O$ (0.1 equiv), sodium ascorbate (0.2 or 0.3 equiv) 1:1 DCM/water; (vi) $[Re(CO)_5Cl]$ (1.0 equiv), toluene, reflux.

separated from the anodic compartment via a glass frit of fine porosity. The counter electrode was a platinum wire gird (10 × 40 mm), and the reference electrode was a saturated Ag/AgCl/KCl electrode that is separated from the solution by a Vycor tip. MeCN solutions containing 0.1 M Bu_4NPF_6 as the supporting electrolyte were saturated with CO_2 for at least 15 min prior to bulk electrolysis and was stirred rigorously during the experiment. Typically, the solution volume of the cathodic compartment was 9 mL with a headspace volume of 50 mL.

Photochemistry. Photochemical reactions were performed using a 300 W, high-pressure Xe arc lamp (Oriel Instruments). The beam was passed through an infrared filter, a collimating lens, and a filter holder equipped with a 415 nm band-pass filter. Samples were prepared in a 1 cm path length quartz cuvette (Starna), which was placed in a temperature-controlled cuvette holder (Quantum Northwest) maintained at 20 °C with a circulated water bath. For the entirety of the study, a MeCN/triethanolamine (TEOA) mixture (5:1 v/v) was used as the solvent. Samples containing 50 μM of Re complex (catalyst), 500 μM of $[Ru(bpy)_3]Cl_2$ (photosensitizer), and 100 mM of BIH (electron donor) were saturated with CO_2 by bubbling CO_2 directly into the solution mixture for 10 min. All samples were assayed under an atmosphere of CO_2. Control experiments in the absence of Re complexes were also performed, and the evolution of the products was subtracted from the experiments containing Re complexes.

Chemical Analysis. H_2 and CO evolution were monitored by gas chromatography during bulk electrolysis and photocatalysis by periodically sampling 50 μL of the headspace. Measurements for H_2 were performed by gas chromatography on a Shimadzu GC-2014 equipped with a Quadrex column, a thermal conductivity detector, and using N_2 as a carrier gas. CO was measured using a Shimadzu GC-2010 Plus gas chromatography, fitted with a Restek Shin Carbon column, helium carrier gas, a methanizer, and a flame ionization detector. Gas chromatography calibration curves were made by sampling known volumes of CO and H_2 gas, respectively. Formate concentration was determined using a Metrohm 883 Basic IC plus ionic exchange chromatography instrument, using a Metrosep A Supp 5 column and a conductivity detector. A typical measurement consists of sampling 200 μL of the reaction mixture, which is diluted 100-fold in deionized 18 MΩ water, followed by a 20 μL injection into the instrument.

■ RESULTS AND DISCUSSION

Synthesis of Ligands and Complexes. Scheme 1 shows the nine $[Re(pyta)(X)(CO)_3]$ and $[Re(tapy)(X)(CO)_3]$ complexes, as well as one $[Re(quinta)(Br)(CO)_3]$ complex (7), where quinta is a 4-(2-quinolyl)-1,2,3-triazole ligand, which have been investigated. When a pyta-based complex is numbered **x**, the corresponding tapy-based complex is numbered **x′**. Some have already been reported and were thus synthesized according to literature procedures.[17,18] The synthesis and characterization of the new ligands and complexes are described in detail in the Experimental section. The pyta-based complexes have different alkyl and aryl substituents at $N1_{triazole}$ (complexes **1**−**4**), differently para-substituted pyridine moieties (complexes **1**, **5**, **6**), or different halide terminal ligands (X = Cl or Br) (complexes **1**, **8**). The tapy-based compounds all contain a dodecyl chain at $C4_{triazole}$ and different X (Cl or Br) ligands (complexes **1′** and **8′**). For comparison we also synthesized and studied the reference $[Re(bpy)(X)(CO)_3]$ complexes **9** and **10**, with X = Cl and Br, respectively, as well as $[Re(quinpy)(Cl)(CO)_3]$ (**11**), where quinpy is a 2-(2-quinolyl)-pyridine ligand.

The ligands were synthesized following the pathways described in Scheme 2. The pyta ligands were synthesized by copper-catalyzed azide−alkyne cycloadditions (CuAAC) using the corresponding azido intermediates and 2-ethynylpyridine derivatives. The different azido intermediates were prepared using standard azidation conditions from the corresponding anilines or by direct substitution of halogen-substituted precursors.[19,20] 2-Ethynyl-4-nitropyridine was prepared from 2-bromo-4-nitropyridine by Sonogashira coupling with triisopropylsilylacetylene followed by triisopropylsilane (TIPS) cleavage using TBAF (33% yield over two steps). Sonogashira coupling with trimethylsilylacetylene afforded instead the tetramethylsilane (TMS)-protected 2-ethynyl-4-nitropyridine in good yield (83%). Subsequent TMS deprotection by treatment with potassium carbonate in methanol led to 2-ethynyl-4-methoxypyridine as the major product (73% isolated yield). The same reactivity was reported by Carlsson et al.[23] during the course of our studies. CuAAC reactions on these derivatives with dodecyl azide afforded ligands for complexes **6** and 7. 2-Pyridin-2-yl-quinoline, the ligand of complex **11**, was synthesized in one step by modifying a previously described Stille coupling procedure using 2-chloroquinoline and 2-(tributylstannyl)pyridine.[27,28] The synthesis of the new complexes followed classical procedures by refluxing the desired ligand with rhenium pentacarbonyl chloride in toluene (Scheme 2).

Single crystals suitable for X-ray diffraction were isolated in the case of complex **3** by slow evaporation of a chloroform solution of the complex. A summary of the crystal data collection and refinement parameters are listed in Table S2. Selected interatomic bond lengths and angles are listed in Table S3. An ORTEP diagram of complex **3** is shown in Figure 1. The Re(I) ion attains the usual distorted octahedral coordination geometry with bond lengths and angles within the typical range found for tricarbonyl rhenium complexes.[13,16,17,29−31] Besides the bidentate pyta ligand, the Re(I) ion has three carbonyl ligands adopting the expected facial arrangement, while the coordinated chloride occupies the other apical position. The Re, C(27), Cl(1), and O(2) atoms are disordered over two sites with occupancies 0.867:0.133. Compared to the structures of related compounds,[30] the dihedral angle between the triazole cycle and the 2,4,6-tri-*tert*-butylphenyl ring is close to 90° and is likely due to the steric influence of the *tert*-butyl groups. This steric bulk also hinders the rotation around the triazole-phenyl bond as reflected by the solution ^{1}H NMR of **3**, where the protons of the *tert*-butyl groups at the 2- and 6-positions of the phenyl ring are no longer equivalent.

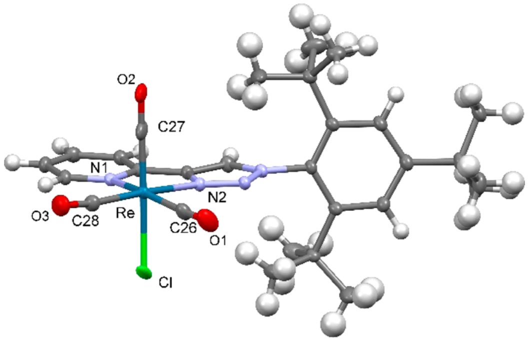

Figure 1. ORTEP plot of 3, with 50% probability thermal ellipsoids and the atom numbering scheme. (Only one of the disordered positions is represented by clarity).

Electrochemical Characterization of the Re Complexes in the Absence of CO_2. The electrochemical behavior of the various complexes, at a concentration of 1 mM, was investigated by cyclic voltammetry (CV) at 100 mV s^{-1} in argon-saturated MeCN in the presence of Bu_4NPF_6 (0.1 M) as the supporting electrolyte, using a glassy carbon electrode. All CVs are shown in the Table S1 and referenced to SCE using Fc/Fc^+ (0.46 V vs SCE) as an internal standard.

Scanning toward positive potentials, a first irreversible oxidation is observed at ∼1.45 V vs SCE, associated with the Re(II)/Re(I) couple, followed by a second oxidation at ∼1.9 V vs SCE, assigned to the oxidation of the ligand.[16] The redox potential values of these features are given in Table S1. Both are only very slightly sensitive to modifications of the ligands: as expected, more positive values are obtained with electron-withdrawing ligands, while less positive values are obtained with electron-donating ligands (compare **5** and **6**, e.g.). Scanning toward negative potentials, an irreversible feature is observed in the case of Re pyta complexes. This feature has been previously assigned to the multielectron reduction of the ligand in DCM.[16] This redox process is more significantly affected by the electronic properties of the ligands (ca. −1.65 V for **1**−**4**; −1.79 V for **5**; −1.08 V for **6** vs SCE). The reduction peak current displays a linear relation to the square root of the scan rate (e.g., Figure S1 for complexes **2** and **3**), indicating that the active species are molecular in nature and that they function in a diffusion-controlled regime. This reduction process was further investigated by rotating disk and microelectrode voltammetry on complex **2** (Figure S2). Solving the Levich−Koutecky equation and the equation for limiting current at a microelectrode simultaneously,[32,33] the diffusion coefficient was found to be 1.6×10^{-5} $cm^2 \cdot s^{-1}$, which is comparable to related complexes.[13,34] The number of electrons for this peak was 1.3 suggesting that this feature in the CV is predominately a one-electron process.

In agreement with tapy ligands having poorer electron-donating ability than the corresponding pyta ligands,[31] the redox features of Re tapy complexes are in general anodically shifted with respect to their corresponding Re pyta complexes (e.g., **1** vs **1′**). In particular, the irreversible cathodic feature was shifted up to almost 200 mV. The same remark must be applied to the $[Re(quinta)(Br)(CO)_3]$ complex (**7**), which has a cathodic feature at −1.29 V vs SCE, in agreement with the quinta ligand being less electron-donating than the corresponding pyta ligand. Furthermore, CVs of Re tapy complexes display an additional feature when scanning further cathodically at ca. −1.64 V vs SCE, which is assigned to a further reduction of the complex. In the case of **6** an additional reversible signal at −0.5 V is assigned to the reversible reduction of the nitro group.

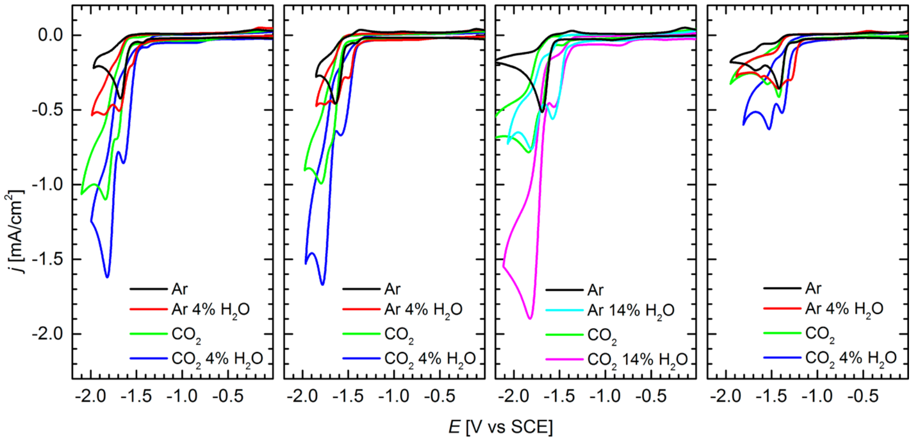

Figure 2. CVs of 1 mM of compounds **1**, **2**, **3**, and **1′** (left to right) in MeCN with 0.1 M Bu_4NPF_6 under argon or CO_2 and with or without water recorded at 0.1 $V \cdot s^{-1}$ at a glassy carbon disk electrode at room temperature.

Reduction of the complexes is also observed to occur at lower potential with X = Cl vs X = Br (compare **1** and **8**).

The well-defined redox events described above are observed in the same potential range as in the CVs of the reference $[Re(bipy)(X)(CO)_3]$ complexes **9**−**10**. However, the reduction of the bipy ligand occurs at much less negative potentials (ca. −1.3 V vs SCE), allowing, as in the case of Re tapy complexes, a second reduction of the complex to occur at ca. −1.5 V vs SCE, in agreement with previous reports.[12,13] Finally, complex **11**, which has a ligand where one of the bipy pyridines has been changed to a quinoline, displays greatly anodically shifted features in its CV (Table S1).

Electrochemical Characterization of the Re Complexes in the Presence of a Proton Source. For Re pyta and Re tapy complexes, the addition of increasing amounts of water results in more complex CVs, notably in the −1.5/−1.8 V vs SCE region (Figure 2, Figures S3), without showing a significant catalytic process. In all cases the first reduction feature occurs at more positive potential, shifting anodically with the amount of water. Furthermore, a new feature appears at ca. −1.8 V vs SCE and increases in intensity upon addition of water. This change was most prominent and resolved for **3**. The titration end point occurred at ∼4%, 6%, and 14% v/v water for **1**, **2**, and **3**, respectively. At saturation, the peak potential of the first reduction wave has shifted by ca. +150 mV in the case of **3** and slightly less for **1** and **2**. The size and shape of the new feature at −1.8 V vs SCE are consistent with a second one-electron process favored by the addition of water. These observations are tentatively interpreted as reflecting first a displacement of the anionic chloride ligand by a neutral aqua ligand thus making the complex more easily reduced (Scheme S1). The same trend has been observed with $[Re(bipy)(X)(CO)_3]$ complexes.[29,35] The irreversibility of the first reduction wave suggests that the aqua ligand decoordinates from the complex as is the case for the halide analogues. Then, the singly reduced complex is protonated, most likely at the triazolyl ligand, favoring a second one-electron reduction. A similar process involving protonation and electron transfer has recently been postulated for a ruthenium polypyridyl complex containing accessible Brønsted base sites.[36] Protonation of the coordinated triazolyl ligand is also suggested by the different water titration end points that were observed for complexes **1**−**3**.

The proposed mechanism shown in Scheme S1 is also supported by CV experiments using trifluoroethanol (TFE) at increasing concentrations up to 1.2% v/v (Figure S4). While the peak potential of the first reduction wave has shifted only slightly, because TFE is a poorer ligand than water, thus less efficient for chloride ligand exchange, a second reduction wave is observed at −1.8 V vs SCE even at this low TFE concentration. This is also consistent with protonation of the complex, facilitating reduction, since TFE (estimated $pK_a^{MeCN} \approx 33.6$[37]) is a stronger Brønsted acid than water ($pK_a^{MeCN} \approx 38{-}41$[37]).

Electrochemical Characterization of the Re Complexes in the Presence of CO_2. Catalytic activity with respect to the electroreduction of CO_2 was first evaluated using CV under conditions described above, but in a CO_2-saturated electrolyte. A catalytic wave is observed in the case of selected Re pyta complexes (Figure 2). In contrast, for reasons requiring further investigations, this wave was much less intense with Re tapy complexes (Figure 2). For this reason, we exclusively studied the former. Furthermore, as the reduction of complex **5** occurs at a more negative potential (−1.8 V), it was not studied further. Complex **6** also did not display any catalytic activity, because its reduction potential is too positive, due to the strong electron-withdrawing power of the nitro substituent on the pyta ligand. Similarly complex **7** does not show any catalytic activity in the range of potentials studied here. Note that this is also the case for compound **11**, indicating that substituting a quinoline moiety for a pyridine in a diimine ligand has a drastically adverse effect on the catalytic activity. Typical experiments are shown in Figure 2, and in all cases (complexes **1**−**3**), in the presence of CO_2, the catalytic wave is observed at a potential more negative (−1.8 V vs SCE) than that corresponding to ligand reduction (ca. −1.65 V vs SCE; Table 1). Interestingly the peak potential corresponds to the second reduction of the complex in the presence of a proton source (see above). Consistently, addition of water has a stimulating effect on the catalytic wave. As seen in Figure 2 and Figure S5, in the case of complexes **1**, **2**, and **4**, the catalytic peak increases upon the addition of more water up to ∼4−5%. Further addition of water has no further effect. In contrast, maximal catalytic peak is obtained with 14% water for complex **3** (Figure 2 and S5). In all cases a noncatalytic prefeature shifting anodically upon the addition of more water is observed. Thus, the reaction occurs via two successive one-electron processes. A first reduction, facilitated by Cl ligand substitution with a molecule of water, generates a one-electron reduced $[Re(L)(CO)_3]$ species, which is not catalytic. Because of protonation of the ligand, which facilitates further reduction, a second electron transfer to the complex, which is required to achieve catalysis, occurs at −1.8 V vs SCE. Thus, the Re pyta complexes can accumulate two electrons and bind CO_2 to achieve a two-electron reduction of CO_2.

Table 1. Comparison of the Catalytic Peak Current (E_c), Overpotential (η), and $(i_c/i_p)^2$ with Proton Sources for Selected Complexes

	proton source (v/v)	E_c (V vs SCE)	η (mV)	$(i_c/i_p)^2$
1	H_2O (4%)	−1.67	690	14
2	H_2O (4%)	−1.64	670	15
3	H_2O (14%)	−1.69	640	12
3	TFE (4.6%)	−1.87	760	176
9		−1.58	570	75

In Table 1 the most active compounds are compared in terms of catalytic peak potential (E_c), overpotential (η), and $(i_c/i_p)^2$, where i_c is the catalytic peak current and i_p is the peak current associated with the catalyst in the absence of substrate. The last quantity, $(i_c/i_p)^2$, is proportional to the turnover frequency (TOF),[34] thus providing a useful benchmark of the relative TOF. These terms are potential-independent in cases where the catalytic current is measured at its plateau value. To calculate the overpotential we compared the standard potential for the CO_2/CO couple in MeCN (−0.89 V vs SCE)[11] to the onset potential extrapolated from the CVs, since CO is to be the major product of the reaction (see below). Thus, Table 1 shows that, in the presence of water, complexes **1**−**3** have similar TOFs and η, with **2** having the best TOF ($(i_c/i_p)^2 = 15$), while **3** has the lowest overpotential (640 mV). In comparison, reference complex **9** is ∼5 times more efficient at ∼100 mV lower overpotential.

Controlled Potential Electrolysis. To further characterize the catalyzed reaction, long-term controlled potential electrolysis (CPE) of CO_2-saturated MeCN/water with 0.1 M

Bu_4NPF_6 was performed using complexes **1**−**3** as well as complex **9** as a reference catalyst. Two different potentials were applied: −1.75 and −1.85 V. While only CO was formed in the case of **9**, as previously reported,[12,13] both CO and H_2 were detected by gas chromatography during CPE in the case of complexes **1**−**3**. No formate was observed by ion-exchange chromatography. Figure S6 shows that, for all the Re pyta complexes, the current density remained approximately constant for 6 h under these conditions. As expected, the current density value is dependent on the applied potential (Figure S6). For complex **1** the current density decreases after ~6 h, while complex **3** remains active for at least 19 h (Figure S7). The stability of the complexes was assessed by electrochemical characterization of the solution during CPE. As shown in Figure S8, the electrochemical signatures of the complexes and the catalytic waves of **1** and **2** have decreased after 8 h CPE, coupled with the appearance of a wave ~1.5 V vs Ag/AgCl. The origins of this feature will require further investigations; nevertheless, its appearance suggests some degradation of complex **1** and **2** during CPE. In contrast, the CVs of complex **3** recorded during CPE were essentially the same, suggesting that it is more stable than **1** and **2** under these conditions.

Faradaic yields (FY) and TONs values for CPE are reported in Table 2. The results show that total FY in most cases are close to 100%. However, significant differences are observed with respect to CO/H_2 ratios between the three Re pyta complexes. While complexes **1** and **2** gave significant amounts of H_2 (FY ≈ 25−45% and CO/H_2 ≈ 1.5−3), complex **3** was much more selective for CO (FY ≈ 80−90% and CO/H_2 ≈ 10), producing both gases at a steady linear rate for 19 h (Figure 3). In comparison, besides being very selective for CO, reference complex **9** was also more efficient. Under similar CPE conditions, complex **9** produced ~3 times more products than the Re pyta complexes.

Table 2. Controlled Potential Electrolysis[a] of 1, 2, 3, and 9 at Different Potentials with Different Proton Sources

	proton source (v/v)	V vs Ag/AgCl	*t* (h)	TON CO	TON H_2	FY (%) CO	FY (%) H_2
1	H_2O (4%)	−1.75	8	3.3	2.5	56	43
		−1.85	6	3.3	1.3	65	26
2	H_2O (4%)	−1.75	8	3.3	1.7	61	31
		−1.85	8	4.7	2.4	52	27
3	H_2O (14%)	−1.75	8	4.7	0.6	89	11
			19	11.5	1.6	81	11
		−1.85	8	5.2	1.2	78	18
3	TFE (4.6%)	−1.75	8	5.0	<0.1	92	<1
		−1.85	8	7.6	0.6	88	7
9	H_2O (4%)	−1.85	4	9.2	<0.1	>99	<1

[a] 1 mM complexes **1**−**3** in CO_2 saturated MeCN with 0.1 M Bu_4NPF_6 using a glassy carbon disk electrode (15 mm dia.) at room temperature.

However, note that systems that produce a mixture of CO and H_2, whose proportions can be controlled, have some value: indeed a mixture of H_2 and CO, also known as syngas, is an attractive feedstock for the chemical industry.[38] Coupling the electrochemical CO_2 reduction to syngas to a subsequent gas-phase catalytic Fischer−Tropsch process step constitutes an alternative strategy to produce synthetic fuels from waste CO_2.

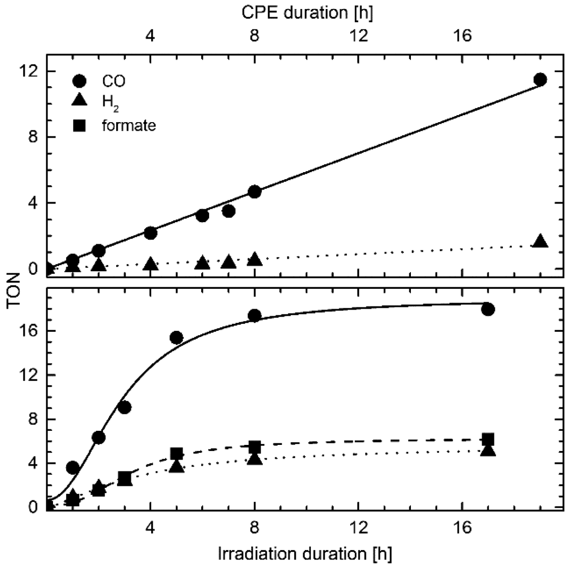

Figure 3. CO (●), H_2 (▲) and formate (■) production during CPE (top) at −1.75 V vs Ag/AgCl catalyzed by 1 mM of complex **3**, in CO_2-saturated MeCN/H_2O (86:14 v/v) with 0.1 M Bu_4NPF_6, using a glassy carbon disk electrode (15 mm diameter) at room temperature; and irradiation (bottom) catalyzed by 0.05 mM of complex **1** in CO_2 saturated MeCN/TEOA (5:1 v/v) with 0.5 mM $[Ru(bpy)_3]Cl_2$ (photosensitizer) and 100 mM BIH (electron donor) using a 300 W Xe arc lamp equipped with a 415 nm filter at 20 °C.

The class of catalysts reported here might be interesting in that respect, since slight modifications of the pyta ligand are significantly impacting the CO/H_2 ratio.

Another way to modulate the CO/H_2 ratio is to change the proton source;[39] thus, the reduction of CO_2 by complex **3** was also studied with the addition of TFE. Figure S9 shows the CV of complex **3** in a CO_2-saturated electrolyte with increasing concentration of TFE. The current of the catalytic wave increases with TFE concentration, reaching a maximum at ~4.6% TFE with a current density of 7.3 mA cm^{-1}. At this concentration of TFE, the $(i_c/i_p)^2$ value is about a magnitude higher than in the case of 14% water, but the overpotential is 120 mV more negative (Table 1). CPE of CO_2-saturated MeCN/TFE with 0.1 M Bu_4NPF_6 was performed using complex **3** at −1.75 and −1.85 V vs Ag/AgCl. Although the $(i_c/i_p)^2$ value derived from the CV with TFE as the proton source is significantly higher, CPE at the less negative potential using 4.6% TFE or 14% water has almost the same TON (5.0 vs 4.7) for CO after 8 h (Table 2), and this can be attributed to the higher overpotential when TFE is used. In contrast, the TON for CO after 8 h of CPE using TFE at the more negative potential is ~50% higher than when water was used (7.6 vs 5.2). Moreover, at a given CPE potential when TFE is used instead of water, a higher CO/H_2 ratio is observed (Table 2), with CPE at −1.75 V vs Ag/AgCl using TFE giving exclusively CO at 92% FY. Finally, in the case of complex **3**, no matter the proton source, it appears that the CO/H_2 can be controlled by the CPE potential, with more H_2 being consistently produced at the more negative potential. Figure 4 summarizes the control one can have over the activity of **3** by changing the potential and the proton source.

Photochemistry. The photoreduction of CO_2 in the presence of **1**−**3** and 1,3-dimethyl-2-phenyl-2,3-dihydro-1*H*-benzo[d]imidazole (BIH), as the electron donor, in MeCN/TEOA was also assessed. Unlike the reference complexes **9** and

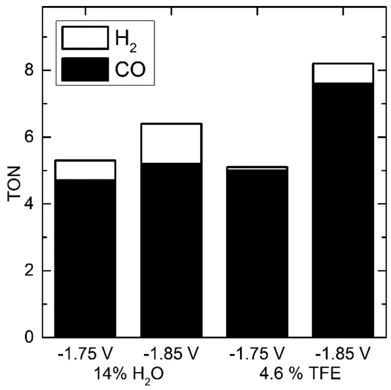

Figure 4. TON for CO (black) and H_2 (white) after 8 h of CPE at −1.75 V or −1.85 V vs Ag/AgCl catalyzed by 1 mM of complex **3**, in CO_2 saturated MeCN with H_2O (14% v/v) or TFE (4.6% v/v) with 0.1 M Bu_4NPF_6, using a glassy carbon disk electrode (15 mm diameter) at room temperature.

10[40] and other mononuclear Rebpy systems,[29,41] no photocatalytic activity was observed for the Re pyta complexes. However, with the addition of $[Ru(bpy)_3]^{2+}$ as a photosensitizer, CO_2 reduction products were readily observed for homogeneous systems containing complexes **1** or **2**. Table 3 shows that upon visible light irradiation, CO, H_2, and formate are produced in the cases of **1** and **2**, while only H_2 is observed for **3**. Complex **1** is the most active, steadily producing CO, H_2, and formate at TOF of 3.0, 0.7, and 1.0 h^{-1}, respectively, for up to 5 h, after which the production levels off (Figure 3). Control experiments in the absence of Re pyta complexes suggest noticeable degradation or deactivation of the photosensitizer after 5 h.

Table 3. Photolytic CO_2 Reduction[a] Using 1−3 as Catalysts

	time plateau (h)	TON			TOF (h^{-1})		
		CO	H_2	formate	CO	H_2	formate
1	5	15	4	5	3.0	0.7	1.0
2	5	12	2	3	2.6	0.6	0.8
3	5	0	3	0		0.6	

[a] 0.05 mM complexes **1**−**3**, with 0.5 mM $[Ru(bpy)_3]Cl_2$ and 100 mM BIH in CO_2 saturated MeCN/TEOA (5:1 v/v) irradiated with a 300 W Xe arc lamp equipped with a 415 nm filter at 20 °C.

Similar to the electrochemical experiments, CO is the major reduction product in the photochemical experiments involving complexes **1** and **2** ($CO/H_2 \approx 3.8–6$). Formate is also produced; however, these values should be considered with caution, because $[Ru(bpy)_2]^{2+}$, a decomposition product of $[Ru(bpy)_3]^{2+}$, can photocatalyze the reduction of CO_2 to formate,[42] and a significant amount is observed in our control experiments. In contrast, complex **3** is inactive in the photoreduction of CO_2 even in the presence of a photosensitizer. This is surprising when considering the similarities between the electrochemical properties of **1**−**3**, and it provides possible insights into the mechanism. The potential of the $[Ru(bpy)_3]^{2+}/[Ru(bpy)_3]^+$ couple ($E_{1/2} = -1.59$ V vs SCE[43]) is just negative enough to reduce complexes **1**−**3** by one electron but is insufficient to doubly reduce them. Therefore, the activity that is observed for complexes **1** and **2** is likely to proceed via a similar mechanism as $[Re(bpy)(CO)_3X]$ complexes, in which a one-electron reduced species (OERS) reacts with CO_2 and receives an electron from another OERS to form a doubly reduced CO_2 adduct.[44] A binuclear intermediate is implied by this mechanism.[45,46] The inactivity of complex **3** in the photochemical experiments supports this proposed mechanism, as the steric hindrance of the tri-*tert*-butyl phenyl moiety near the Re active site would hamper the formation of the binuclear intermediate.

Previous studies have also shown that $[Re(bpy)(CO)_3\{R_2N-CH_2CH_2O-COO\}]$ (where R = CH_2CH_2OH) is an important adduct in photocatalytic systems using $[Re(bpy)(CO)_3X]$ in CO_2-saturated DMF/TEOA solutions and is believed to be applicable to Re(I)-diimine complexes in general.[47] Although MeCN and not DMF is used as the solvent in the present work, it is likely that the formation of the TEOA-CO_2 adduct is still an important factor. Therefore, the steric hindrance in complex **3** may also have impeded the formation of the active TEOA-CO_2 adduct and resulted in inactivity.

■ CONCLUSION

A new series of well-characterized Re pyta and Re tapy tricarbonyl complexes have been studied for their ability to catalyze the electro- and photoreduction of CO_2. We specifically investigated the influences of the two isomeric pyridyl−triazolyl ligands and of functionalizing the pyridyl and triazolyl rings on their catalytic activity. On the one hand, although the Re tapy derivatives (**1′** and **8′**) displayed similar CV features as the reference complexes **9** and **10**, they do not show appreciable activity for the reduction of CO_2. On the other hand, for Re pyta derivatives (**1**−**4**) that display a first reduction wave at ∼1.7 V vs SCE, a catalytic wave is observed in the presence of CO_2. Changing the potential of this reduction wave by the introduction of electron-donating (**5**, **7**) or electron-withdrawing (**6**) groups on the pyridyl ring results in decreased activity. The first reduction wave is also influenced by the auxiliary halide ligand (**1** vs **8**), and from the CVs of **1**−**3** in the presence of water it is likely that an aqua ligand displaces the coordinated halide. The added water also acts as a proton source facilitating a second reduction of the complex at slightly more negative potential. For the active complexes, addition of a proton source also enhanced the catalytic wave that is observed in the presence of CO_2. While by no means outperforming complex **9**, the catalytic rates for complexes **1**−**3** in the presence of water (4 or 14%) were only ∼5 times slower, with ∼100 mV higher overpotential. For complex **3** the addition of 4.6% TFE increases the catalytic rate by over a magnitude but at a cost of another 100 mV overpotential. CPE experiments using **1**−**3** in the presence of a proton source show that CO is the major product of the electrocatalytic reaction, with complex **3** displaying the best stability (19 h) and selectivity for CO (up to 92% FY). In contrast, complex **3** does not catalyze the reduction of CO_2 in photocatalytic experiments using $[Ru(bpy)_3]^{2+}$ as a photosensitizer, whereas complexes **1** and **2** display good activity, producing ∼13 TON of CO as the major product over the course of 5 h. Currently, we are exploiting our ability to dis-symmetrically furnish functional groups on the pyta scaffold to (i) better understand and improve the catalytic efficiency and selectivity of this new class of CO_2 reduction catalyst; and (ii) graft the catalyst onto the surface of conductive materials for the manufacturing of solid electrodes, the results of which will be reported in due course.

ASSOCIATED CONTENT

Supporting Information

The Supporting Information is available free of charge on the ACS Publications website at DOI: 10.1021/acs.inorgchem.6b03078.

X-ray crystallographic information (CIF)

Proposed reduction mechanism, CVs, illustrated structures, selected potentials, tabulated crystallographic data and structure refinement details, selected experimental bond lengths and angles, plots of current densit as a function of time, photo of experimental setup with parts labeled (PDF)

AUTHOR INFORMATION

Corresponding Authors

*E-mail: clotilde.policar@ens.fr. (C.P.)
*E-mail: fethi.bedioui@chimie-paristech.fr. (F.B.)
*E-mail: marc.fontecave@college-de-france.fr. (M.F.)

ORCID

Clotilde Policar: 0000-0003-0255-1650
Marc Fontecave: 0000-0002-8016-4747

Notes

The authors declare no competing financial interest.

CCDC 1518528 contains the supplementary crystallographic data for this paper. These data can be obtained free of charge from the Cambridge Crystallographic Data Centre via http://www.ccdc.cam.ac.uk/Community/Requestastructure.

ACKNOWLEDGMENTS

We acknowledge PSL Research University ("PSL-Chimie" Project CATACARB under the Framework Agreement ANR-10-IDEX-0001-02) for funding. The China Scholarship Council for a CSC scholarship for M.H. The authors would like to thank Dr. P. Simon (College de France) for assistance with gas and ion chromatography, and Dr. V. Mougel (College de France), Dr. Maria Gomez-Mingot (College de France), and T. Forgeron (College de France) for fruitful discussions.

REFERENCES

(1) Rakowski Dubois, M.; Dubois, D. L. Development of Molecular Electrocatalysts for CO 2 Reduction and H 2 Production/Oxidation. *Acc. Chem. Res.* **2009**, *42* (12), 1974−1982.

(2) Morris, A. J.; Meyer, G. J.; Fujita, E. Molecular Approaches to the Photocatalytic Reduction of Carbon Dioxide for Solar Fuels. *Acc. Chem. Res.* **2009**, *42* (12), 1983−1994.

(3) Benson, E. E.; Kubiak, C. P.; Sathrum, A. J.; Smieja, J. M. Electrocatalytic and Homogeneous Approaches to Conversion of CO2 to Liquid Fuels. *Chem. Soc. Rev.* **2009**, *38* (1), 89−99.

(4) Qiao, J.; Liu, Y.; Hong, F.; Zhang, J. A Review of Catalysts for the Electroreduction of Carbon Dioxide to Produce Low-Carbon Fuels. *Chem. Soc. Rev.* **2014**, *43* (2), 631−675.

(5) Rodrigues, N. P.; Obirai, J.; Nyokong, T.; Bedioui, F. Electropolymerized Pyrrole-Substituted Manganese Phthalocyanine Films for the Electroassisted Biomimetic Catalytic Reduction of Molecular Oxygen. *Electroanalysis* **2005**, *17* (2), 186−190.

(6) Harrison, D. P.; Lapides, A. M.; Binstead, R. A.; Concepcion, J. J.; Méndez, M. A.; Torelli, D. A.; Templeton, J. L.; Meyer, T. J. Coordination Chemistry of Single-Site Catalyst Precursors in Reductively Electropolymerized Vinylbipyridine Films. *Inorg. Chem.* **2013**, *52* (9), 4747−4749.

(7) Blakemore, J. D.; Gupta, A.; Warren, J. J.; Brunschwig, B. S.; Gray, H. B. Noncovalent Immobilization of Electrocatalysts on Carbon Electrodes for Fuel Production. *J. Am. Chem. Soc.* **2013**, *135* (49), 18288−18291.

(8) Chen, X.; Ren, H.; Peng, W.; Zhang, H.; Lu, J.; Zhuang, L. Highly Efficient Molecular Cobalt Electrode for (Photo)electrochemical Hydrogen Evolution. *J. Phys. Chem. C* **2014**, *118* (36), 20791−20798.

(9) Elgrishi, N.; Griveau, S.; Chambers, M. B.; Bedioui, F.; Fontecave, M. Versatile Functionalization of Carbon Electrodes with a Polypyridine Ligand: Metallation and Electrocatalytic H + and CO 2 Reduction. *Chem. Commun.* **2015**, *51* (14), 2995−2998.

(10) Rosser, T. E.; Windle, C. D.; Reisner, E. Electrocatalytic and Solar-Driven CO 2 Reduction to CO with a Molecular Manganese Catalyst Immobilized on Mesoporous TiO 2. *Angew. Chem., Int. Ed.* **2016**, *55* (26), 7388−7392.

(11) Costentin, C.; Drouet, S.; Robert, M.; Savéant, J.-M. A Local Proton Source Enhances CO2 Electroreduction to CO by a Molecular Fe Catalyst. *Science* **2012**, *338* (6103), 90−94.

(12) Hawecker, J.; Lehn, J.-M.; Ziessel, R. Electrocatalytic Reduction of Carbon Dioxide Mediated by Re(bipy) (CO)3Cl (Bipy = 2,2?-Bipyridine). *J. Chem. Soc., Chem. Commun.* **1984**, *984* (6), 328.

(13) Smieja, J. M.; Kubiak, C. P. Re(bipy-tBu) (CO)3Cl-Improved Catalytic Activity for Reduction of Carbon Dioxide: IR-Spectroelectrochemical and Mechanistic Studies. *Inorg. Chem.* **2010**, *49* (20), 9283−9289.

(14) Smith, A. P.; Fraser, C. L. Bipyridine Ligands. In *Comprehensive Coordination Chemistry II*; Elsevier, 2003; Vol. *1*, pp 1−23.

(15) Bodapati, R.; Sarma, M.; Kanakati, A.; Das, S. K. Asymmetrically Substituted and π-Conjugated 2,2′-Bipyridine Derivatives: Synthesis, Spectroscopy, Computation, and Crystallography. *J. Org. Chem.* **2015**, *80* (24), 12482−12491.

(16) Kim, T. Y.; Elliott, A. B. S.; Shaffer, K. J.; John McAdam, C.; Gordon, K. C.; Crowley, J. D. Rhenium(I) Complexes of Readily Functionalized Bidentate Pyridyl-1,2,3-Triazole "click" ligands: A Systematic Synthetic, Spectroscopic and Computational Study. *Polyhedron* **2013**, *52*, 1391−1398.

(17) Bertrand, H. C.; Clède, S.; Guillot, R.; Lambert, F.; Policar, C. Luminescence Modulations of Rhenium Tricarbonyl Complexes Induced by Structural Variations. *Inorg. Chem.* **2014**, *53* (12), 6204−6223.

(18) Clède, S.; Lambert, F.; Saint-Fort, R.; Plamont, M. A.; Bertrand, H.; Vessières, A.; Policar, C. Influence of the Side-Chain Length on the Cellular Uptake and the Cytotoxicity of Rhenium Triscarbonyl Derivatives: A Bimodal Infrared and Luminescence Quantitative Study. *Chem. - Eur. J.* **2014**, *20* (28), 8714−8722.

(19) Gjonaj, L.; Roelfes, G. Selective Chemical Modification of DNA with Alkoxy- and Benzyloxyamines. *Org. Biomol. Chem.* **2015**, *13* (21), 6059−6065.

(20) Juríček, M.; Kouwer, P. H. J.; Rehák, J.; Sly, J.; Rowan, A. E. A Novel Modular Approach to Triazole-Functionalized Phthalocyanines Using Click Chemistry. *J. Org. Chem.* **2009**, *74* (1), 21−25.

(21) Zhu, X. Q.; Zhang, M. T.; Yu, A.; Wang, C. H.; Cheng, J. P. Hydride, Hydrogen Atom, Proton, and Electron Transfer Driving Forces of Various Five-Membered Heterocyclic Organic Hydrides and Their Reaction Intermediates in Acetonitrile. *J. Am. Chem. Soc.* **2008**, *130* (8), 2501−2516.

(22) Bolje, A.; Urankar, D.; Košmrlj, J. Synthesis and NMR Analysis of 1,4-Disubstituted 1,2,3-Triazoles Tethered to Pyridine, Pyrimidine, and Pyrazine Rings. *Eur. J. Org. Chem.* **2014**, *2014* (36), 8167−8181.

(23) Carlsson, A.-C. C.; Mehmeti, K.; Uhrbom, M.; Karim, A.; Bedin, M.; Puttreddy, R.; Kleinmaier, R.; Neverov, A. A.; Nekoueishahraki, B.; Gräfenstein, J.; Rissanen, K.; Erdélyi, M. Substituent Effects on the [N−I−N] + Halogen Bond. *J. Am. Chem. Soc.* **2016**, *138* (31), 9853−9863.

(24) Sheldrick, G. M. *SHELXS-97, Program for Crystal Structure Solution*; University of Göttingen: Göttingen, Germany, 1997.

(25) Sheldrick, G. M. *SHELXL-97*, Program for the Refinement of Crystal Structures from Diffraction Data; University of Göttingen: Göttingen, Germany, 1997.

(26) Farrugia, L. J. Suite for Small-Molecule Single-Crystal Crystallography. *J. Appl. Crystallogr.* **1999**, *32* (4), 837−838.

(27) Tsuboyama, A.; Okada, S.; Takiguchi, T.; Suzuki, K.; Miura, S.; Moriyama, T.; Igawa, S.; Kamatani, J.; Furugori, M.; Iwawaki, H. Electroluminescent Device Using Metal Coordination Compound. US 2004/0013905 A1, Jan. 22, 2004.

(28) Combs, A. P.; Sparks, R. B.; Maduskuie, T. P., Jr.; Rodgers, J. D. Tricyclic Heterocycles as BET Protein Inhibitors. WO2014/143768 A1, Sept 18, 2014.

(29) Kurz, P.; Probst, B.; Spingler, B.; Alberto, R. Ligand Variations in $[ReX(diimine)(CO)_3]$ Complexes: Effects on Photocatalytic CO_2 Reduction. *Eur. J. Inorg. Chem.* **2006**, *2006* (15), 2966−2974.

(30) Wolff, M.; Munoz, L.; François, A.; Carrayon, C.; Seridi, A.; Saffon, N.; Picard, C.; Machura, B.; Benoist, E. Tricarbonylrhenium Complexes from 2-Pyridyl-1,2,3-Triazole Ligands Bearing a 4-Substituted Phenyl Arm: A Combined Experimental and Theoretical Study. *Dalton Trans.* **2013**, *42* (19), 7019−7031.

(31) Lo, W. K. C.; Huff, G. S.; Cubanski, J. R.; Kennedy, A. D. W.; McAdam, C. J.; McMorran, D. A.; Gordon, K. C.; Crowley, J. D. Comparison of Inverse and Regular 2-Pyridyl-1,2,3-triazole "click" Complexes: Structures, Stability, Electrochemical, and Photophysical Properties. *Inorg. Chem.* **2015**, *54* (4), 1572−1587.

(32) Bard, A. J.; Faulkner, L. R. *Electrochemical Methods,* 2nd ed.; John Wiley & Sons, Ltd, 2001.

(33) Baur, J. E.; Wightman, R. M. Diffusion Coefficients Determined with Microelectrodes. *J. Electroanal. Chem. Interfacial Electrochem.* **1991**, *305* (1), 73−81.

(34) Smieja, J. M.; Sampson, M. D.; Grice, K. A.; Benson, E. E.; Froehlich, J. D.; Kubiak, C. P. Manganese as a Substitute for Rhenium in CO_2 Reduction Catalysts: The Importance of Acids. *Inorg. Chem.* **2013**, *52* (5), 2484−2491.

(35) Johnson, F. P. A.; George, M. W.; Hartl, F.; Turner, J. J. Electrocatalytic Reduction of CO_2 Using the Complexes $[Re(bpy)(CO)_3L]^N$ (N = + 1, L = $P(OEt)_3$, CH_3CN; N = 0, L = Cl^-, Otf^-; Bpy = 2,2′-Bipyridine; Otf^- = CF_3SO_3) as Catalyst Precursors: Infrared Spectroelectrochemical Investigation. *Organometallics* **1996**, *15* (15), 3374−3387.

(36) Saravanan, K.; Keith, J. A. Standard Redox Potentials, pK_aS, and Hydricities of Inorganic Complexes under Electrochemical Conditions and Implications for CO_2 Reduction. *Dalt. Trans* **2016**, *45* (39), 15336−15341.

(37) Felton, G. A. N.; Vannucci, A. K.; Okumura, N.; Lockett, L. T.; Evans, D. H.; Glass, R. S.; Lichtenberger, D. L. Hydrogen Generation from Weak Acids: Electrochemical and Computational Studies in the $[(\eta^5\text{-}C_5H_5)Fe(CO)_2]_2$ System. *Organometallics* **2008**, *27* (18), 4671−4679.

(38) Foit, S.; Eichel, R.-A.; Vinke, I. C.; de Haart, L. G. J. Power-to-Syngas - an Enabling Technology for the Transition of the Energy System? Production of Tailored Synfuels and Chemicals Using Renewably Generated Electricity. *Angew. Chem., Int. Ed.* **2016**, 1 DOI: 10.1002/anie.201607552.

(39) Liyanage, N. P.; Dulaney, H. A.; Huckaba, A. J.; Jurss, J. W.; Delcamp, J. H. Electrocatalytic Reduction of CO_2 to CO With Re-Pyridyl-NHCs: Proton Source Influence on Rates and Product Selectivities. *Inorg. Chem.* **2016**, *55* (12), 6085−6094.

(40) Hawecker, J.; Lehn, J.-M.; Ziessel, R. Efficient Photochemical Reduction of CO_2 to CO by Visible Light Irradiation of Systems Containing $Re(bipy)(CO)_3X$ or $Ru(bipy)_3^{2+} - Co^{2+}$ Combinations as Homogeneous Catalysts. *J. Chem. Soc., Chem. Commun.* **1983**, No. 9, 536−538.

(41) Hori, H.; Ishitani, O.; Koike, K.; Johnson, F. P. A.; Ibusuki, T. Efficient Carbon Dioxide Photoreduction by Novel Metal Complexes and Its Reaction Mechanisms. *Energy Convers. Manage.* **1995**, *36* (6−9), 621−624.

(42) Hawecker, J.; Lehn, J.-M.; Ziessel, R. Photochemical Reduction of Carbon Dioxide to Formate Mediated by Ruthenium Bipyridine Complexes as Homogeneous Catalysts. *J. Chem. Soc., Chem. Commun.* **1985**, *20* (2), 56.

(43) Juris, A.; Balzani, V.; Belser, P.; von Zelewsky, A. Characterization of the Excited State Properties of Some New Photosensitizers of the Ruthenium (Polypyridine) Family. *Helv. Chim. Acta* **1981**, *64* (7), 2175−2182.

(44) Takeda, H.; Koike, K.; Inoue, H.; Ishitani, O. Development of an Efficient Photocatalytic System for CO_2 Reduction Using Rhenium(I) Complexes Based on Mechanistic Studies. *J. Am. Chem. Soc.* **2008**, *130* (6), 2023−2031.

(45) Gibson, D. H.; Yin, X. Synthesis and Reactions of Fac-$Re(dmbpy)(CO)_3X$ (Dmbpy = 4,4′-Dimethyl-2,2′-Bipyridyl; X = COOH, COOMe, H, OH, and OCHO). *J. Am. Chem. Soc.* **1998**, *120* (43), 11200−11201.

(46) Hayashi, Y.; Kita, S.; Brunschwig, B. S.; Fujita, E. Involvement of a Binuclear Species with the Re−C(O)O−Re Moiety in CO_2 Reduction Catalyzed by Tricarbonyl Rhenium(I) Complexes with Diimine Ligands: Strikingly Slow Formation of the Re−Re and Re−C(O)O−Re Species from $Re(dmb)(CO)_3S$ (Dmb = 4,4′-Dimethyl-2. *J. Am. Chem. Soc.* **2003**, *125* (39), 11976−11987.

(47) Morimoto, T.; Nakajima, T.; Sawa, S.; Nakanishi, R.; Imori, D.; Ishitani, O. CO_2 Capture by a Rhenium(I) Complex with the Aid of Triethanolamine. *J. Am. Chem. Soc.* **2013**, *135* (45), 16825−16828.